

# Mantled alkali-feldspar megacrysts from the marginal part of the Karkonosze granitoid massif (SW Poland)

EWA SŁABY<sup>1</sup>, LUIZA GALBARCZYK-GĄSIOROWSKA<sup>1</sup> & ANNA BASZKIEWICZ<sup>2</sup>

<sup>1</sup>*Institute of Geochemistry, Mineralogy and Petrology of the Warsaw University, Al. Żwirki i Wigury 93, PL-02-089 Warszawa, Poland. E-mails: eslaby @ geo.uw.edu.pl; luiza@geo.uw.edu.pl*

<sup>2</sup>*Polskie Górnictwo Naftowe S.A., ul. Jagiellońska 76, PL-03-301 Warszawa, Poland. E-mail: anna.baszkievicz@pgnig.com.pl*

## ABSTRACT:

SŁABY, E., GALBARCZYK-GĄSIOROWSKA, L. & BASZKIEWICZ A. 2002. Mantled alkali-feldspar megacrysts from the marginal part of the Karkonosze granitoid massif (SW Poland). *Acta Geologica Polonica*, **52** (4), 501-519. Warszawa.

Mantled alkali feldspar megacrysts from the porphyritic granite variety of the Karkonosze Variscan pluton (SW Poland) have been studied. The feldspars contain numerous inclusions of minerals (mainly plagioclases), which form inner rims, marking successive zones of megacryst growth, and they are surrounded by a plagioclase mantle (rapakivi texture). Although, due to maturation and coarsening, the feldspars display a heterogeneous exsolution pattern, in the core part some homogeneous sectors (without visible decomposition) are also preserved. Chemical composition of alkali feldspar megacrysts (including barium concentration) and of plagioclases (inner inclusions and mantle) has been determined and used for evaluation of thermal conditions of melt crystallization. The highest calculated temperature for single equilibrium and close-to-equilibrium pairs of un-decomposed domains in alkali feldspar + plagioclase inclusion ranges 809-750°C. The differences in crystallization temperature calculated for the pairs alkali feldspar domains (megacryst) and plagioclase inclusions from successive inner rims or for the pairs alkali feldspar domains (megacryst) – plagioclase mantle varied within 100°C. Common lack of equilibrium for neighbouring pairs of plagioclase inclusion – alkali feldspar is noticeable. Growth morphologies of plagioclases (inclusions and mantle) and alkali feldspar have been proved by means of CL. Mostly the feldspars display signs of resorption and re-growth at many stages of their formation. The barium concentration in the feldspars also points to discontinuous growth. The crystallization path of the megacrysts and the formation of rapakivi texture were influenced by magma mixing, not by decompression processes.

**Key words:** Mantled minerals, Rapakivi texture, Magma mixing, Geothermometry, Cathodoluminescence of feldspar minerals, Karkonosze pluton.

## THE AIM OF THE WORK

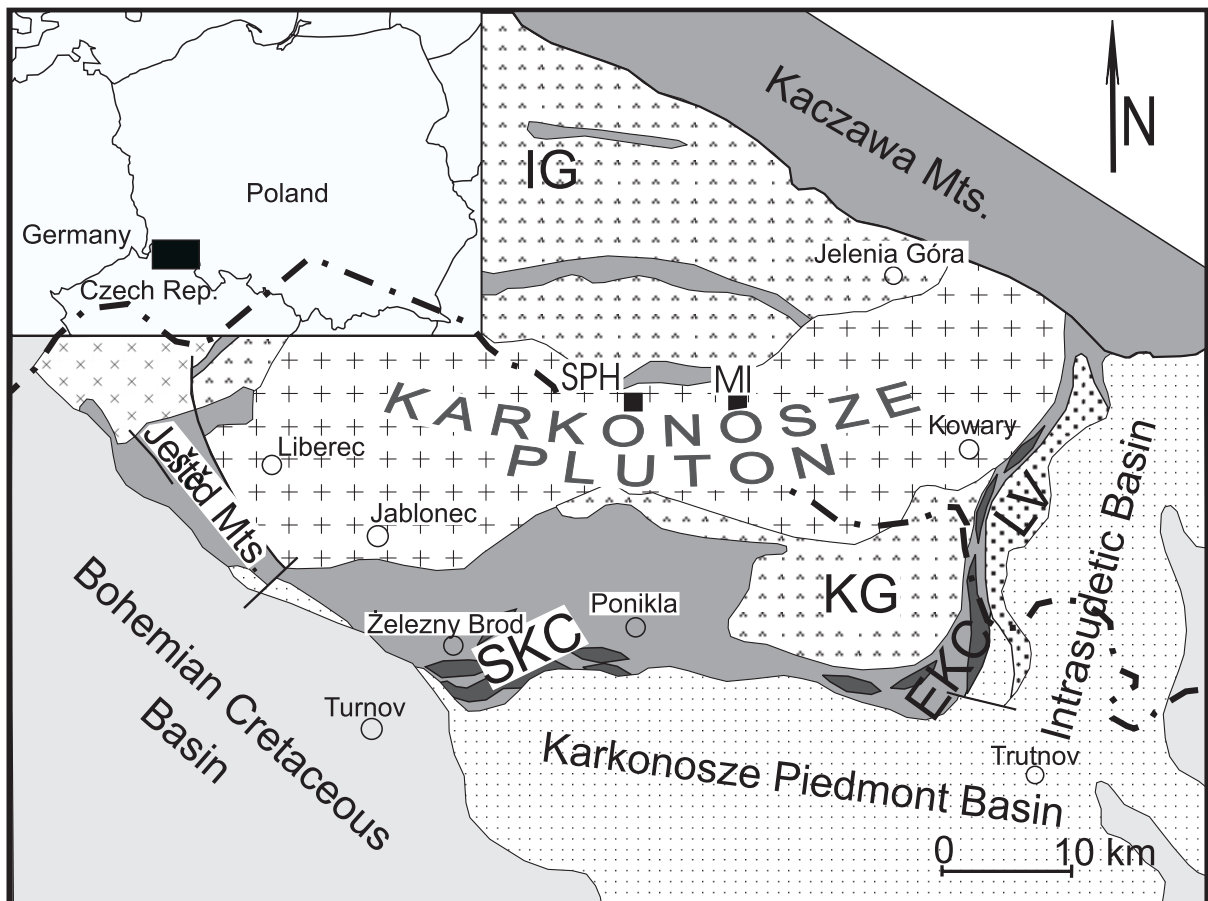
Mantled feldspars (rapakivi) belong to textures interpreted usually as compatible with magma mixing (HIBBARD 1981, BUSSY 1990, WARK & STIMAC 1992, MÜLLER & SELTMANN 2001). Open system processes are not the only ones forming the rapakivi. The texture is also often referred to in connection with the decom-

pression and undercooling process during the magma ascent (CHERRY & TREMBATH 1978; NEKVASIL 1991; EKLUND & SHEBANOV 1999). The Karkonosze granitic pluton consists of several facies, with the porphyritic facies predominating. The latter contains alkali feldspar megacrysts mantled with plagioclases, which resemble those of rapakivi granites. The aim of the work is to characterise the growth morphology and the

composition of the feldspars in order to reconstruct the steps of their textural evolution and the thermal conditions of their crystallization. The alkali feldspar megacrysts seem to be an especially good subject for the estimation of crystallization temperature. They are not only surrounded by a plagioclase mantle but they contain many plagioclase inclusions. The pairs alkali feldspar domain + plagioclase could then give valuable information about the crystallization temperature of selected parts of the megacryst. The main objective is to arrive at conclusions regarding the origin of the rapakivi texture.

## GEOLOGICAL SETTING

Geologically, the Sudetes lie between the NW-SE Odra Elbe Fault Zones on the NE margin of Bohemian Massif, forming the eastern extremity of the European Variscan belt (ALEKSANDROWSKI & *al.* 2000). The area comprises two domains: West Sudetic with a prevailing NW-SE structural grain and East Sudetic with a NNE-SSW structural trend. The Karkonosze-Izera Massif with the late- (WILAMOWSKI 1998) to postorogenic granite pluton (DIOT & *al.* 1994, 1995; DUTHOU & *al.* 1991) belongs to the West Sudetic domain (Text-fig. 1). The West




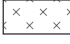

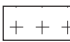

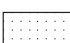



- |   |   |   |   |
|---|---|---|---|
|  | low-grade metasediments with subordinate metavolcanics                                    |  | Late Proterozoic and Cambria/Ordovician granitoids        |
|  | medium-grade metasediments and metagranitoids   |  | Variscan granitoids                                       |
|  | low-grade metamorphosed volcano-sedimentary sequences with abundant bimodal metavolcanics |  | Carboniferous and Permian syn- and post-orogenic deposits |
|  | low- to medium-grade metamorphosed volcano-sedimentary sequences dominated by mafic rocks |  | Mesozoic platform deposits                                |
|   |   |  | Polish - Czech border                                     |

Fig. 1. Simplified geological map of Karkonosze-Izera massif (after PATOČKA & *al.* 2000); IG – Izera gneisses and granito-gneisses with mica schist belts, EKC – East Karkonosze Complex, LV – Leszczyniec unit, SKC – South Karkonosze Complex; SPH – Szklarska Poręba Huta, MI – Michałowice quarries

porphyritic granite), a ridge granite and a granophyric granite. According to KLOMINSKY (1969) four types of biotite granite, two-mica granite, and three types of granodiorite within the Karkonosze pluton could be distinguished.

Mantled alkali feldspar megacrysts appear mainly in the porphyritic granite. Rare plagioclase megacrysts have been also reported from the granite. Apart from the megacrysts, the occurrence of numerous biotite schlieren and enclaves in the rock is a key characteristic of the porphyritic granite type. The porphyritic granite type is a typical subsolvus, two-feldspar granite. The content of three main components varies strongly in the granite from one outcrop to the other: 22-40% for quartz, 19-35% for alkali feldspar, 25-39% for plagioclase (BORKOWSKA 1966). The main mafic mineral is biotite. The biotite content usually does not exceed 6%, but in the biotite – rich variety it reaches 22%. The granite includes also small amounts (< 1%) of muscovite, hornblende, epidote, Fe-Ti oxides, zircon, apatite, titanite and, rarely fluorite. The megacrysts, in the biotite - rich variety, are commonly orientated and accompanied by biotite schlieren. The schlieren appear also in the parts depleted in phenocrysts. In many places they are cut by aplitic veins or accompanied by pegmatitic nests. The porphyritic rock bears numerous enclaves, mainly of dioritic and granodioritic composition. A detailed description of the modal composition of many of them points to various degrees of hybridisation (SŁABY 2002), although they have been considered as “reworked” xenoliths in granite melt (BORKOWSKA 1966).

The K-feldspar megacrysts form thick, pink plates or ovoids (the size usually ranges from 2 to 6 cm) very often surrounded by a white, plagioclase rim of 3-4 mm thickness, resembling rapakivi texture (BORKOWSKA 1966). The megacrysts contain numerous, inclusions of biotite, quartz and plagioclase; of these, the biotite is visible macroscopically. The inclusions usually form rings separating the core from the rim of the feldspar. A second generation of alkali feldspar, plagioclase, quartz and hydrous ferromagnesian minerals fill, the space between the megacrysts, producing a medium-grained granitic texture. As a result of the cooling process, many features related to the conditions of primary crystallization have been obscured. The megacrysts show exsolution and alteration microtextures. The matrix feldspars are accompanied by the formation of myrmekite. Some of the plagioclase inclusions in the megacrysts as well as the groundmass plagioclases have been altered due to deuteric processes, of which sericitization and albitization are common. Primary features however, preserved in selected domains of the megacrysts as well as in the matrix crys-

tals, have recorded the early history. BORKOWSKA (1966), in her comprehensive work on Karkonosze granitoid petrology, pointed to different order-disorder of the megacryst structure in comparison with the much smaller alkali feldspars growing as matrix crystals. Similarly, she showed that the two generations of alkali feldspar had a different composition.

The temperature of crystallization of the Karkonosze pluton has been estimated many times before. BORKOWSKA (1966), using the BARTH two – feldspar thermometer (BARTH 1955, 1962) determined the crystallization temperature range to between 730-510°C (the last one clearly influenced by post-magmatic processes). The value was higher for megacrysts in contact with plagioclase than for the second generation of alkali feldspars accompanied by plagioclases. The feldspar analyses were performed on single megacrysts as well as on separates of the second generation of alkali feldspars. The plagioclases analyses were also done on separates. Taking into account the higher Ba content and the less ordered structure of the megacrysts compared with the matrix alkali feldspars, BORKOWSKA (1966) concluded that the megacrysts crystallized earlier. At the same time she assessed the highest possible thermal conditions of the melt crystallization as 750°C at a pressure of 3 kbars using WINKLER'S (1962) anticipation. The contact parageneses found in hornfelses were used for the estimation of the temperature of the granitic melt. OBERC-DZIEDZIC (1985) made use of the paragenesis cordierite+sillimanite+hercynite+corundum+andalusite appearing in the proximity of the contact with the Karkonosze pluton, whose crystallization temperature was not higher than 660°C. This temperature correlates well with the maximum value obtained by BORKOWSKA for the megacrysts, taking into consideration the thermal conductivity of the envelope rocks (OBERC-DZIEDZIC, 1985). The most recent data on the thermal conditions of melt crystallization were provided by isotopic study. Due to limited hydrothermal activity, biotite altered to chlorite has preserved the original magmatic isotope composition during the postmagmatic evolution of pluton (WILAMOWSKI 2002). The composition has been calculated using biotite-water oxygen and hydrogen fractionation for an assumed crystallization temperature of 600°C and equilibrium conditions during oxygen and hydrogen exchange. Received data from slightly chloritised biotite fall into the field of primary magmatic water withholding the assumption as reliable.

The knowledge about rapakivi granite genesis has made considerable progress since M. BORKOWSKA published her views on the genesis of the Karkonosze granite. It is of great interest to look again at the mantled feldspars in the context of possible undercooling processes or open system processes.

within the successive zones bordered by plagioclase inclusions rims. Recapitulating in the alkali feldspar exsolution-free and exsolution-rich domains could be distinguished.

The composition of the megacrysts from both quarries shows some differences and similarities (Text-fig. 2a, b).

The data points split clearly into two groups, although the compositions of the decomposed and un-decomposed parts are similar for both the SPH and MI megacrysts. The content of the orthoclase component in the exsolution-free or almost exsolution-free domains ranges: 65-77 mol % for SPH and 60-80 mol % for MI. The composition of

| Alkali feldspars (SPH)           |                                     |        |        |           |        | Plagioclase inclusions (SPH) |         |        | Plagioclase mantle (SPH) |         |         |         |
|----------------------------------|-------------------------------------|--------|--------|-----------|--------|------------------------------|---------|--------|--------------------------|---------|---------|---------|
| SiO <sub>2</sub>                 | Marginal part to plagioclase mantle |        |        | Core part |        |                              | 63.329  | 61.348 | 61.231                   | 65.341  | 65.320  | 65.800  |
|                                  | 64.948                              | 64.663 | 64.629 | 64.207    | 64.580 | 63.633                       |         |        |                          |         |         |         |
| Al <sub>2</sub> O <sub>3</sub>   | 18.431                              | 18.167 | 18.111 | 18.359    | 18.318 | 18.639                       | 22.991  | 24.322 | 22.733                   | 21.265  | 21.878  | 21.236  |
| CaO                              | 0.000                               | 0.000  | 0.000  | 0.013     | 0.028  | 0.000                        | 4.496   | 5.360  | 6.025                    | 2.927   | 3.236   | 2.544   |
| BaO                              | 0.000                               | 0.000  | 0.000  | 0.578     | 0.331  | 1.939                        | 0.091   | 0.088  | 0.035                    | 0.081   | 0.000   | 0.000   |
| Na <sub>2</sub> O                | 0.258                               | 0.804  | 0.734  | 0.823     | 1.074  | 0.368                        | 8.929   | 8.331  | 7.760                    | 10.032  | 9.823   | 10.230  |
| K <sub>2</sub> O                 | 16.289                              | 15.602 | 15.622 | 15.254    | 14.901 | 15.776                       | 0.204   | 0.270  | 0.102                    | 0.309   | 0.234   | 0.168   |
| total                            | 99.926                              | 99.236 | 99.096 | 99.234    | 99.233 | 100.355                      | 100.039 | 99.719 | 97.885                   | 100.255 | 100.491 | 100.068 |
| Formula recalculated to 8 oxygen |                                     |        |        |           |        |                              |         |        |                          |         |         |         |
| Si                               | 3.001                               | 3.005  | 3.007  | 2.993     | 2.999  | 2.970                        | 2.800   | 2.731  | 2.772                    | 2.874   | 2.864   | 2.892   |
| Al                               | 1.004                               | 0.995  | 0.993  | 1.009     | 1.003  | 1.025                        | 1.198   | 1.276  | 1.213                    | 1.118   | 1.131   | 1.104   |
| Ca                               | 0.000                               | 0.000  | 0.000  | 0.001     | 0.001  | 0.000                        | 0.213   | 0.256  | 0.292                    | 0.138   | 0.152   | 0.120   |
| Ba                               | 0.000                               | 0.000  | 0.000  | 0.011     | 0.006  | 0.035                        | 0.002   | 0.002  | 0.001                    | 0.001   | 0.000   | 0.000   |
| Na                               | 0.023                               | 0.072  | 0.066  | 0.074     | 0.097  | 0.033                        | 0.765   | 0.719  | 0.681                    | 0.855   | 0.835   | 0.872   |
| K                                | 0.960                               | 0.925  | 0.927  | 0.907     | 0.883  | 0.939                        | 0.011   | 0.015  | 0.006                    | 0.017   | 0.013   | 0.009   |
|                                  | 4.988                               | 4.997  | 4.993  | 4.995     | 4.989  | 5.002                        | 4.989   | 4.998  | 4.965                    | 5.003   | 4.995   | 4.997   |

| Alkali feldspars (MI)            |                                     |         |        |           |        | Plagioclase inclusions (MI) |         |         | Plagioclase mantle (MI) |         |        |        |
|----------------------------------|-------------------------------------|---------|--------|-----------|--------|-----------------------------|---------|---------|-------------------------|---------|--------|--------|
| SiO <sub>2</sub>                 | Marginal part to plagioclase mantle |         |        | Core part |        |                             | 68.688  | 69.364  | 69.076                  | 62.977  | 60.471 | 61.374 |
|                                  | 65.756                              | 65.513  | 64.548 | 65.387    | 64.134 | 63.456                      |         |         |                         |         |        |        |
| Al <sub>2</sub> O <sub>3</sub>   | 18.208                              | 18.396  | 18.136 | 18.622    | 18.519 | 18.411                      | 19.588  | 19.291  | 19.220                  | 23.299  | 24.435 | 23.790 |
| CaO                              | 0.000                               | 0.000   | 0.000  | 0.062     | 0.000  | 0.128                       | 0.108   | 0.581   | 0.788                   | 4.626   | 6.299  | 5.366  |
| BaO                              | 0.088                               | 0.175   | 0.433  | 1.463     | 1.564  | 0.845                       | 0.026   | 0.000   | 0.000                   | 0.016   | 0.061  | 0.067  |
| Na <sub>2</sub> O                | 1.101                               | 0.420   | 0.869  | 4.144     | 0.463  | 1.163                       | 11.590  | 10.996  | 11.106                  | 9.120   | 7.788  | 8.601  |
| K <sub>2</sub> O                 | 14.900                              | 15.879  | 15.106 | 9.917     | 15.030 | 14.078                      | 0.246   | 0.103   | 0.100                   | 0.279   | 0.384  | 0.111  |
| total                            | 100.053                             | 100.383 | 99.092 | 99.595    | 99.710 | 98.081                      | 100.546 | 100.336 | 100.290                 | 100.317 | 99.438 | 99.309 |
| Formula recalculated to 8 oxygen |                                     |         |        |           |        |                             |         |         |                         |         |        |        |
| Si                               | 3.018                               | 3.009   | 3.005  | 2.994     | 2.989  | 2.986                       | 2.989   | 3.013   | 3.007                   | 2.782   | 2.743  | 2.707  |
| Al                               | 0.985                               | 0.996   | 0.998  | 1.014     | 1.017  | 1.021                       | 1.005   | 0.988   | 0.986                   | 1.213   | 1.253  | 1.289  |
| Ca                               | 0.000                               | 0.000   | 0.003  | 0.000     | 0.000  | 0.006                       | 0.019   | 0.027   | 0.037                   | 0.219   | 0.257  | 0.302  |
| Ba                               | 0.002                               | 0.003   | 0.000  | 0.018     | 0.029  | 0.016                       | 0.000   | 0.000   | 0.00                    | 0.000   | 0.001  | 0.001  |
| Na                               | 0.098                               | 0.037   | 0.068  | 0.068     | 0.042  | 0.106                       | 0.978   | 0.926   | 0.937                   | 0.781   | 0.745  | 0.676  |
| K                                | 0.872                               | 0.931   | 0.912  | 0.878     | 0.894  | 0.845                       | 0.014   | 0.006   | 0.006                   | 0.016   | 0.006  | 0.022  |
|                                  | 4.975                               | 4.976   | 4.986  | 4.972     | 4.971  | 4.980                       | 5.005   | 4.959   | 4.972                   | 5.011   | 5.005  | 4.997  |

Table 1. Analysis of feldspars from SPH and MI



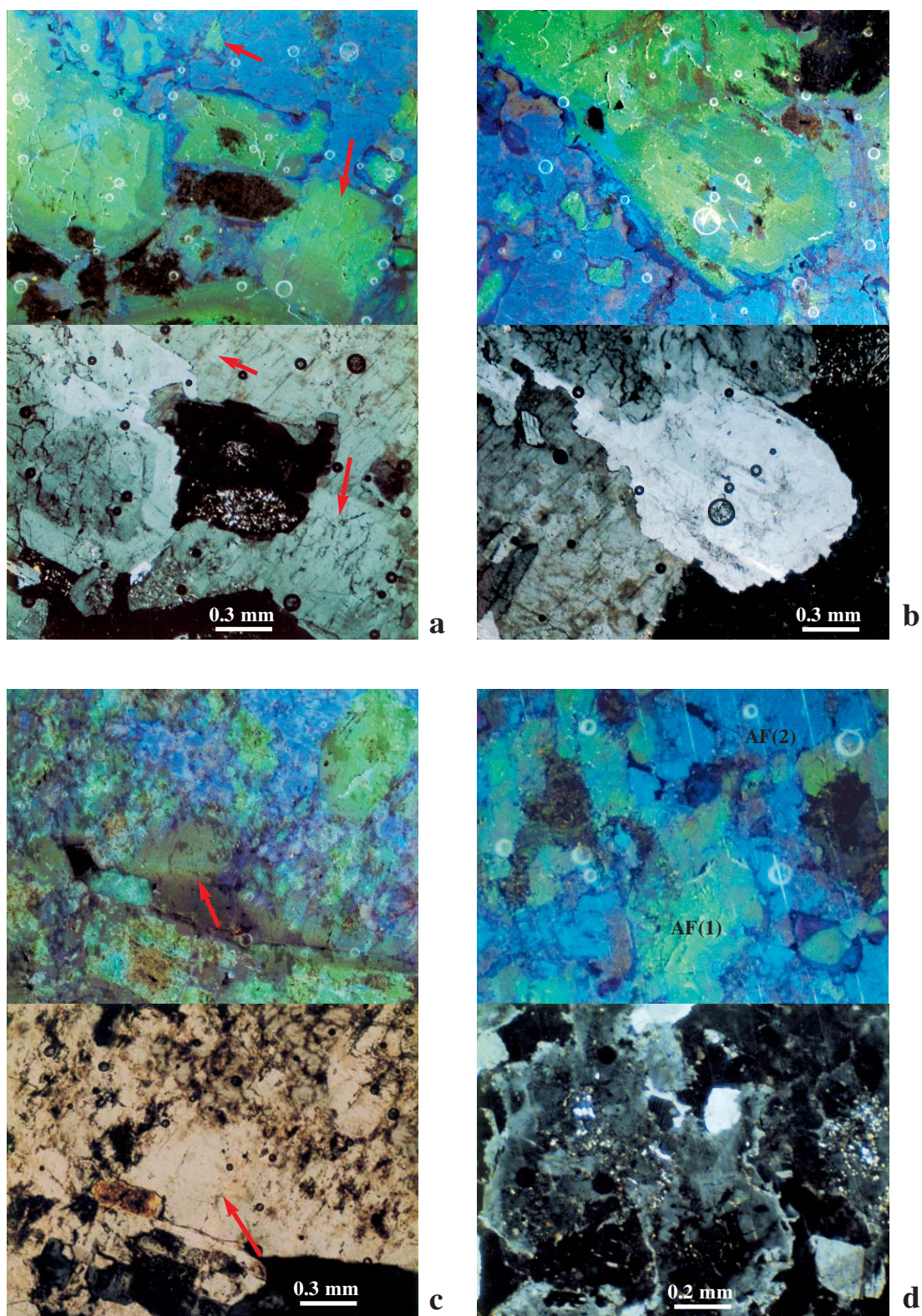


Fig. 4. Pairs of thin section images (crossed nicols – lower photo, cathodoluminescence – upper photo) of alkali feldspar megacryst from SPH; a – part close to plagioclase mantle, arrows pointed to relics of resorbed plagioclases, invisible under crossed nicols; b – inner plagioclase surrounded by small relics of resorbed plagioclase integrated to growing alkali feldspar; c – marginal part of alkali feldspar depleted in trace elements (arrow); d – zone of alkali feldspar between two inner plagioclase rims composed from homogeneous parts (AF2) and parts composed of mixtures of incompletely resorbed plagioclase with overgrowing alkali feldspar (AF1)

### *Plagioclase*

Two generations of plagioclase occur in the rock. The first one appears as inclusions in the megacrysts, the second one forms a mantle on the megacrysts and crystallise together with the other matrix minerals. The internal morphology and composition of both generations is different.

### *Plagioclase inclusions in alkali feldspar*

Plagioclases appearing inside alkali feldspar megacrysts form single, irregular patches in the centre or gather along a line, forming a zone. The zone marks successive stages of alkali feldspar growth (Text-fig. 3 a, b). Close to the rapakivi mantle, the plagioclase inclusions appear in the form of irregular spots with corroded boundaries. Euhedral shape is rare. The growth morphology of all of the plagioclases shows a complex core with concordant rims. It suggests some stages of discontinuation of growth, dissolution and re-growth. Some examples of plagioclase internal morphology are shown in Text-fig. 5. The same plagioclases are shown as crossed – polarized and CL (cathodoluminescence) micrographs. The chemistry and mode of feldspar occurrences is reflected by the luminescence colour (MARSHALL 1988, RAMSAYER & *al.*, 1992, RAMSEYER & MULLIS 2000). The parts of the MI granitic plagioclase enriched in anorthite show bluish colours, whereas the albite-rich parts show pinkish-brown colours. For the albite-rich parts the possible activators are iron atoms (GÖTZE & *al.* 2000), as confirmed in the present study by microprobe analysis. CL pictures show a complicated crystallization path of those plagioclases. Dissolution textures as well as re-growth of melted parts can often be recognized only on the CL images (Text-fig. 5a-d). The plagioclases display at least 4 stages of crystallization (Text-fig. 5a). The crystals are often interlarded with apatite needles. The albite-rich plagioclase rim is accompanied by small veins, which contact the rim and are filled with small crystals of the same composition (Text-fig. 5b, c). In many cases the rim does not present a homogeneous zone, but contains many crystals of the same composition (usually albite-oligoclase). This pattern is also accompanied by fractures, where plagioclase continued to crystallize (Text-fig. 5c). The centres of some plagioclase reveal irregularly distributed small spots, which are composed of a mixture of minerals (Text-fig. 5b). The mixture has blue-greenish flaming luminescence. Minute Ca-bearing crystals are recognised within the mixture indicating anorthite-rich prior plagioclase sectors or they may be melt inclusion. Rims and

patches of irregular forms surround the partly melted and recrystallized crystal core. The albite-enriched patches, sometimes of euhedral to subhedral shape crystallize close to the resorbed, more basic parts of the core (Text-fig. 5b). Sometimes the albite-enriched patches form a core of plagioclase with concordant, reverse zoning. Plagioclase with such a core appears close to the other one with a complex core and discordant, normal zones. The signs of dissolution and precipitation can also be seen along compositional plane in the twins (Text-fig. 5d). The parted crystal is reconnected by alkali feldspar.

The range of compositional variability is different for the SPH and MI samples (Text-fig. 2). Whereas in the SPH samples the composition of the plagioclase inclusions covers the whole range Ab80-Ab99, the plagioclase analyses from the MI samples split into two groups. The first one is close to the interval Ab65-Ab70, the second close to Ab95. There is a compositional gap between both populations. Furthermore the plagioclases from MI are more basic.

### *Plagioclase mantle*

The mantle of the alkali feldspar megacrysts comprises many crystals, partly penetrating the megacryst itself (Text-fig. 3a). The texture resembles intergrowths. Crystals growing directly on the alkali feldspar surface posse almost the same orientation. The next generation growing on the plagioclases attached to the alkali feldspar, usually includes quartz. The mutual orientation of the crystals is different. The plagioclases growing on the alkali feldspar surface usually show simple concordant zoning, seldom discontinuous. The core, as well as the rims, is often euhedral. The composition of the plagioclase from the SPH samples is more acid than that of the plagioclases appearing as inclusions in the alkali feldspar megacrysts (Text-fig. 2). The core usually displays an anorthite content not higher than 17%, whereas the core of plagioclase inclusion is approximately twice as rich in that component. Plagioclases mantling the MI megacrysts are more basic. In some cases, their cores are enriched in an anorthite component up to 54%, so they are more basic than the plagioclase inclusions in the megacryst. The composition of the MI plagioclases spans the range Ab58-Ab95, with a small gap between Ab46-Ab58. In some of them (MI) small inclusions of alkali feldspars are present. The crystals of alkali feldspars are homogeneous, without exsolutions (Or92Ab8An0 – Or97Ab3An0).

The composition as well as internal morphology, of the plagioclase forming the rapakivi mantle is similar to that of the matrix plagioclase.

| MI   | Nekvasil & Burnham 1987 |         |         |         | Fuhrman & Lindsley 1988 |         |         |         |
|--|-------------------------|---------|---------|---------|-------------------------|---------|---------|---------|
|  | Tab                     | Tor     | Tan     | T       | Tab                     | Tor     | Tan     | T       |
| Alkali feldspar megacryst - homogeneous domains + plagioclase inclusions |                         |         |         |         |                         |         |         |         |
| C-EQ pair  |                         |         |         |         | 809/802                 | 764/766 | 809/802 | 809/802 |
| N-EQ pair  | 838/804                 | 744/732 | 842/804 | 840/804 |                         |         |         |         |
| Alkali feldspar megacryst non-homogenized + plagioclase inclusions       |                         |         |         |         |                         |         |         |         |
| EQ pair  |                         |         |         |         | 403/434                 | 403/417 | 403/434 | 403/434 |
|  |                         |         |         |         | /385                    | /385    | /385    | /385    |
| C-EQ pair  |                         |         |         |         | 466/398                 | 429/450 | 466/450 | 466/424 |
|  |                         |         |         |         | 411/400                 | 459/437 | 459/437 | 435/418 |
| N-EQ pair  | 506/496                 | 327/315 | 506/496 | 506/496 |                         |         |         |         |
|  | 472/466                 | 369/362 | 472/466 | 472/466 |                         |         |         |         |
|  | 471/463                 | 357/345 | 471/463 | 471/463 |                         |         |         |         |
| Alkali feldspar megacryst homogenised + mantle plagioclase               |                         |         |         |         |                         |         |         |         |
| C-EQ pair  |                         |         |         |         | 710/710                 | 678/679 | 710/710 | 710/710 |
| N-EQ pair  | 692/668                 | 612/598 | 692/668 | 692/668 | 670/653                 | 607/605 | 670/653 | 670/653 |
|  | 665/648                 | 513/514 | 665/648 | 665/648 | 612/600                 | 559/555 | 612/600 | 612/600 |
|  | 617/609                 | 467/441 | 617/609 | 617/609 | 777/796                 | 662/640 | 777/796 | 777/796 |
|  | 802/771                 | 551/603 | 802/771 | 802/771 | 745/760                 | 660/664 | 745/760 | 745/760 |
|  | 731/710                 | 602/595 | 731/710 | 731/710 |                         |         |         |         |
| Alkali feldspar megacryst non-homogenised + mantle plagioclase           |                         |         |         |         |                         |         |         |         |
| EQ pair  | 416/560                 | 416/560 | 416/560 | 416/560 | 617/642                 | 617/642 | 629/642 | 623/642 |
|  | 569/547                 | 569/547 | 569/547 | 569/547 | 593/580                 | 576/574 | 593/580 | 596/580 |
|  | 559/                    | 559/    | 559/    | 559/    | 596/551                 | 596/541 | 596/551 | 596/551 |
|  |                         |         |         |         | 571/                    | 554/    | 571/    | 571/    |
| C-EQ pair  | 655/642                 | 618/609 | 655/642 | 655/642 |                         |         |         |         |
| N-EQ pair  | 625/608                 | 526/491 | 625/608 | 625/608 | /586                    | /494    | /494    | /586    |
|  | 490/603                 | 414/517 | 490/603 | 490/603 |                         |         |         |         |
|  | /575                    | /458    | /575    | /575    |                         |         |         |         |
| Alkali feldspar megacryst - perthites                                    |                         |         |         |         |                         |         |         |         |
| EQ pair  | 448/435                 | 454/440 | 454/440 | 454/437 | 381/358                 | 381/358 | 381/358 | 381/358 |
|  | 442/                    | 442/    | 442/    | 442/    | 322/333                 | 322/333 | 322/333 | 322/333 |
|  |                         |         |         |         | 344/318                 | 344/318 | 344/318 | 344/318 |
|  |                         |         |         |         | 341/339                 | 341/339 | 341/339 | 341/339 |
|  |                         |         |         |         | 396/                    | 396/    | 396/    | 396/    |
| C-EQ pair  | 440/358                 | 362/330 | 440/358 | 440/358 |                         |         |         |         |
|  | 366/                    | 342/    | 359/    | 360/    |                         |         |         |         |
|  | 430/                    | 338/    | 430/    | 430/    |                         |         |         |         |
|  | 365/                    | 317/    | 322/    | 343/    |                         |         |         |         |
| N-EQ pair  | 426/362                 | 327/302 | 426/362 | 426/362 | 339/330                 | 428/421 | 428/421 | Recryst |
|  | 431/418                 | 334/329 | 431/418 | 431/418 | 340/328                 | 421/412 | 421/412 | Recryst |
|  | 421/425                 | 355/326 | 421/425 | 421/425 | 347/336                 | 411/402 | 411/402 | Recryst |
|  | 426/420                 | 333/319 | 426/420 | 426/420 |                         |         |         |         |
|  | 433/422                 | 344/333 | 433/422 | 433/422 |                         |         |         |         |
|  | /423                    | /293    | /423    | /423    |                         |         |         |         |
|  | /357                    | /306    | /330    | /357    |                         |         |         |         |
| Matrix alkali feldspar (with perthites) + matrix plagioclase             |                         |         |         |         |                         |         |         |         |
| EQ pair  | 487/477                 | 487/477 | 487/477 | 487/477 | 427/403                 | 427/403 | 427/403 | 427/403 |
|  | 461/454                 | 461/454 | 461/454 | 461/454 | 431/423                 | 431/423 | 431/423 | 431/423 |
|  | 492/479                 | 492/479 | 492/479 | 492/479 | 382/                    | 382/    | 382/    | 382/    |
|  | 496/483                 | 496/483 | 496/483 | 496/483 | 390/                    | 390/    | 390/    | 390/    |
|  |                         |         |         |         | 408/                    | 408/    | 408/    | 408/    |
| C-EQ pair  | 489/                    | 445/    | 489/    | 489/    |                         |         |         |         |
|  | 476/                    | 420/    | 476/    | 476/    |                         |         |         |         |
| N-EQ pair  | 474/                    | 455/    | 474/    | 474/    |                         |         |         |         |
|  | 476/                    | 449/    | 476/    | 476/    |                         |         |         |         |
| Matrix plagioclases with alkali feldspars inclusions                     |                         |         |         |         |                         |         |         |         |
| EQ pair  | 402/410                 | 402/410 | 402/410 | 402/410 | 321/322                 | 321/322 | 321/322 | 321/322 |
|  | 302/296                 | 302/296 | 302/296 | 302/296 |                         |         |         |         |
|  | 452/437                 | 452/437 | 452/437 | 452/437 |                         |         |         |         |
|  | 460/444                 | 460/444 | 460/444 | 460/444 |                         |         |         |         |
|  | 307/299                 | 307/299 | 307/299 | 307/299 |                         |         |         |         |
|  | 409/405                 | 409/405 | 409/405 | 409/405 |                         |         |         |         |

Explanation: EQ / C-EQ / N-EQ: equilibrium, close to equilibrium, non-equilibrium pair; the first value calculated to 3 kbars, the second for 2 kbars pressure.



For the calculations the most external zone of plagioclase has been used in every case. The more basic cores of the plagioclases gave the higher temperatures, but the origin of these cores has been disputable. From their composition it is probable, that they crystallized in the magma chamber. It cannot be however excluded, that they have been brought with a magma injection of different origin.

The thermal conditions accompanying the coarsening process in the SPH and MI granites were similar to each other. Often for the adjacent domains of exsolved feldspar discordant temperatures are obtained from the models. The process seems to be obscured by hydrothermal recrystallization. The coarsening started generally below 500 °C although some single pairs are close to equilibrium above this temperature and terminate around 320 °C. Similar temperatures have been obtained for the pairs matrix alkali feldspar (with perthite) – matrix plagioclase or matrix plagioclase together with alkali feldspar inclusions entirely surrounded by plagioclase. All of the pairs gave perfect by concordant temperatures, which did not exceed 500 °C using the NEKVASIL & BURNHAM model and showed strongly non-equilibrium behaviour in the FUHRMAN & LINDSLEY model.

## DISCUSSION AND CONCLUSIONS

The appearance of mantled alkali feldspar megacryst in the Karkonosze granite could have resulted either from magma-mixing or from changes in crystallization conditions during magma emplacement.

### **Magma mixing as a process potentially responsible for rapakivi texture formation**

Many observations argue in favour of the magma mixing hypothesis. The most important are: textures observed in the feldspars, trace element composition of the alkali feldspar megacrysts, presence of hybridised enclaves, reconstructed thermal conditions of magma crystallization.

Textures found in the megacrysts and also in other minerals could indicate a mixing system. Many of the alkali feldspar megacrysts (but not all) show a plagioclase mantle (rapakivi texture). The texture of the megacrysts displays often an advanced stage of development in a mixing system. Although finally euhedral, with the mantle composed of plagioclases and quartz, they exhibit an ovoidal core surrounded by a poly-mineral inclusions rim and many zones of more or less euhedral shape bordered by mineral inclusions. Single crystals of quartz show poikilitic texture with corroded

biotite, plagioclase and earlier quartz generation relics. The quartz relics are surrounded by sub-microscopic, minute rims of other minerals, reminiscent of ocellar texture (KLAR 1986, ŚLABY 2002).

Feldspars from both porphyritic granites (SPH and MI) display resorption textures. Although plagioclase mantled megacrysts do not show the classic dendritic morphology, they form several, irregular patches in the K-feldspar interior. These patches join the mantle. HIBBARD (1981) interpreted similar textures as having been developed in a hybrid rock resulting from magma mixing. The zone including plagioclase patches contains hidden, abundant traces of dissolved plagioclases (compare the CL images) and textures showing dissolution of alkali feldspars. That the traces of dissolved plagioclases are still visible, may perhaps be due to preserved  $Me^{+2}$  activators, which previously replaced calcium in the plagioclase (GÖTZE & *al.* 2000). The zone does not present the typical bladed or cellular forms described by WARK & STIMAC (1992), but the textures observed in the SPH and MI samples suggest inward growth of the plagioclases. The habit and frequency of plagioclase inclusions in the alkali feldspar interior could also bear testimony to mixing. Some of the plagioclases have anorthite-rich cores. These cores show many stages of dissolution and regrowth, which could point to hybridisation of the granite magma by a basic magma. The successive rims of plagioclase inclusions in the megacrysts might correspond to successive pulses of basic magma.

The barium distribution in the alkali feldspar megacrysts could be another indicator of magma mixing. Because the diffusivity of Ba is very low, the zoning represents primary composition (AFONINA & SHMAKIN 1970). Barium decreases with differentiation in felsic rocks, reflecting the timing of K-feldspar crystallization (MCINTIRE 1963, LONG & LUTH 1986). The zoning pattern for the two-phase system: alkali feldspar-melt ( $D_{Ba}^{af/liq} > 1$ ) is normal, although it depends strongly on the amount of the crystalline phase in the system and the barium partitioning between crystal and melt, which is in turn temperature dependent (LONG & LUTH 1979, 1986). Simultaneously, crystallization of additional phases (plagioclase  $D_{Ba}^{pl/liq} < 1$ , quartz  $D_{Ba}^{q/liq} = 0$ ), together with alkali feldspar, behaviour of barium, causing its elevated concentration in the residual liquid and reverse Ba zoning in the alkali feldspar (WHITNEY 1975). The crystallization path of the granite melt depends on water content in the melt, which also influences the barium distribution. LONG and LUTH (1986) showed in their simulation that a 2% difference in water content changes the order of crystallization, and produces different Ba-zoning profiles. A low water content (2 wt%) favours plagioclase crystallization, which reduces the ability of the alkali feldspar to take up



the magmatic conditions of the formation of the megacrysts. In our case the anticipation is difficult. The evaluation of crystallization temperature could be burdened with inaccuracies at various stages of the operation. Mostly the data are calculated for reconstructed alkali feldspar composition. Many of the thermal data lie above, many below the minimum eutectic value. It indicates re-equilibration. The data could be valuable if we assume that the reconstruction of the primary composition of every zone within the megacryst is equally uncertain and that the kinetic of the maturation process of the zones has been similar within one megacryst. It is difficult to judge whether or not the reconstructed composition of the alkali feldspar corresponds to the primordial, magmatic one. We believe that, although in some places the inter-exchange between plagioclases and alkali feldspars under subsolidus conditions could have been possible, the pairs show mostly the primary composition, modified by recrystallization rather than by interdiffusion. The first one seems to affect recrystallization at some places only the marginal parts of the alkali feldspars. Because the reconstructed compositions gave crystallization temperatures between the values of strain-free solvus and coherent solvus we decided to use the data for the estimation of relative changes in the thermal conditions of magma crystallization.

The information about the thermal conditions of crystallization of successive zone obtained from the profile along the whole megacryst indicates surprisingly small differences between the calculated temperatures (maximum around 80°C). The temperatures denote, however, not the temperatures relating to the point of the magma mixing process itself, but to the re-equilibration of the system after mixing. We also do not know the temperature of megacryst nucleation. Due to the presence of inclusions in the alkali feldspar crystals we are able to estimate the temperature of alkali feldspar – plagioclase re-equilibration after every magma mixing event, assuming that every inclusion zones originated from the change in the order of mineral crystallization caused by mafic magma injection. Under this assumption, the obtained information shows the relative differences in the re-equilibration temperature of magma crystallization after every mixing event.

#### **Decompression as a process responsible for rapakivi texture formation**

Taking into account the thermal history of the SPH and MI granite crystallization, the ascent of the magma took place with a loss of temperature. The last stage of alkali feldspar crystallization and the plagioclase

mantling was accompanied by immense resorption of plagioclase (CL images) and less pronounced resorption of alkali feldspar. Simultaneous resorption of both feldspars is possible under isothermal decompression (NEKVASIL 1991). The difference between temperatures of the formation of the pair alkali feldspar megacryst – plagioclase inclusions varies within the range 100 °C. The difference in crystallization temperatures of the pairs alkali feldspar megacryst – external plagioclase rim and matrix alkali feldspar – matrix plagioclase reaches 70°C. Ascent of natural magmas results in a small temperature loss, 3–7°C/kbar (RUMBLE 1976, SYKES & HOLLOWAY 1987). Assuming a heat loss of 7°C/kbar, only slight rounding of plagioclase may take place. At a cooling rate higher than 10 °C/kbar, resorption of plagioclase is impossible (NEKVASIL 1991). Additionally, the juxtaposed thermal profile for successive plagioclase inclusion zones points to multiple increase and decrease in crystallization temperature.

One of the features of the rapakivi texture formed under decompression should be a small compositional change between the first and second generation of feldspars (STEWART 1959, BLADH 1980). The observed compositional differences in the SPH and MI feldspars are too big to be considered alone as a result of perturbation during decompression. According to NEKVASIL (1991), the alkali feldspar after decompression should show a reduced Or content. On the contrary, alkali feldspars from both the SPH and MI sites (margin parts of megacrysts and the groundmass feldspars) are enriched in the Or component. The enrichment might, however, be the result of reworking by hydrothermal fluids.

Taking into account the thermal history of the evolution of the megacrysts, their chemical composition as well as their textural features, it seems that the mantled feldspars were formed as a result of magma mixing.

MÜLLER and SELTMANN (2001, in press) and SELTMANN & *al.* 2001) reported on the Altenberg-Frauenstein rapakivi granite, the only one known from the German-Czech part of the and the only one known at the eastern extremity of the Variscan belt. They enumerated some features after HAAPALA and RÄMÖ's definition of rapakivi granite (HAAPALA & RÄMÖ 1992, RÄMÖ & HAAPALA 1995). All of the the specified features are similar to those of the Karkonosze porphyritic granite type. As in the case of the Altenberg-Frauenstein rapakivi granite, the central and ridge granite from the Karkonosze pluton show features of "A-type" post-collisional granite (WHALEN & *al.* 1987) displaying in some varieties the rapakivi texture (DOMAŃSKA & *al.* 2002). The composition shows high tFe/(Mg+tFe) in mafic minerals, high K-feldspar content and acid plagioclases

- the Proterozoic rapakivi granites of southeastern Fennoscandia. *Transactions of the Royal Society of Edinburgh: Earth Sciences*, **83**, 165-171.
- HIBBARD, M.J. 1981. The magma mixing origin of mantled feldspar. *Contributions to Mineralogy and Petrology*, **76**, 158-170.
- 1995. Petrography to petrogenesis. *Prentice-Hall*; New Jersey.
- KACHLIK, V. & PATOČKA, F. 1998. Cambrian/Ordovician intra-continental rifting and Devonian closure of the rifting generated basins in the Bohemian Massif realms. *Acta Universitatis Carolinae – Geologica*, **43**, 433-441.
- KLAR, A. 1986. Stochastic model of Karkonosze granitoid crystallization in area near Szklarska Poręba, Sudetes Mts., South-Western Poland. *Prace Mineralogiczne*, **76**, 1-69. [*In Polish*]
- KLOMINSKY, J. 1969. Krkonosko-jizersky granitoid massif. *Sbornik Geologickich Ved, Geologie*, **15**, 7-132. [*In Czech*]
- KOSSMAT, F. 1927. Gliederung des varistischen Gebirgsbaues. *Abhandlungen Sächsischen Geologischen Landesamts*, **1**, 1-39.
- KROLL, H., EVANGELAKAKIS, C., VOLL, G. 1993. Two feldspar geothermometry: a review and revision for slowly cooled rocks. *Contributions to Mineralogy and Petrology*, **114**, 510-518.
- KRYZA, R. & PIN, C. 1997. Cambrian/Ordovician magmatism in the Polish Sudetes: no evidence for subduction-related setting. In "Abstract Supplement 1, EUG9", Strasbourg, *Terra Nova*, **9**, 144.
- KRYZA R. & MAZUR S. 1995. Contrasting metamorphic paths in the eastern margin of the Karkonosze-Izera Block, SW Poland. *Neues Jahrbuch für Mineralogie, Abhandlungen*, **169**, 157-192.
- LEE, M.R., WALDRON, K.A. & PARSONS, I. 1995. Exsolution and alteration microtextures in alkali feldspar phenocrysts from the Shap granite. *Mineralogical Magazine*, **59**, 63-78.
- LONG, P.E. & LUTH, W.C. 1979. Petrogenesis of microcline megacrysts from Precambrian granitic rocks of the Dixon-Penasco area, northern New Mexico. In: R.V. INGERSOLL (Ed.), *New Mexico Geological Society Guidebook*, 30<sup>th</sup> Field Conference, Sante Fe Country, 145-153.
- & — 1986. Origin of K-feldspar megacrysts in granitic rocks: Implication of a partitioning model for barium. *American Mineralogist*, **71**, 367-375.
- LÓPEZ MORO, F.J., LÓPEZ PLAZA, M. & MARTIN POZAS, J.M. 1998. Characterization and origin of the alkali feldspar of granitoid rocks from the Variscan Anatectic Tormes Dome (West-Central Spain). *European Journal of Mineralogy*, **10**, 535-550.
- MARSHALL, D.J. 1988. Cathodoluminescence of geological material. *Allen & Unwin*; London.
- MATTE, P. 1991. Accretionary history and crustal evolution of the Variscan Belt in Western Europe. *Tectonophysics*, **196**, 309-337.
- MATTE, P., MALUSKI, H., RAJLICH, P., FRANKE, W. 1990. Terrane boundaries in the Bohemian Massif: results of large-scale Variscan shearing. *Tectonophysics*, **177**, 151-170.
- MAZUR, S. 1995. Structural and metamorphic evolution of the country rocks at the eastern contact of the Karkonosze granite in the southern Rudawy Janowickie Mts and Lasocki Ridge. *Geologia Sudetica*, **29**, 31-98.
- 2002. Geology of the Karkonosze-Izera Massif: an overview. *Mineralogical Society of Poland Special Papers*, **20**, 22-34.
- MCINTIRE, W.L. 1963. Trace element partition coefficients – A review of theory and applications to geology. *Geochimica and Cosmochimica Acta*, **27**, 1209-1264.
- MÜLLER, A. & SELTMANN, R. 2001. Textural and mineral-chemical evidence of an Upper Carboniferous rapakivi granite in Erzgebirge /Krusne Hory. In: PIESTRZYŃSKI & *al.* (Eds), *Mineral Deposits at the Beginning of the 21<sup>st</sup> Century. Proceedings of the Joint Sixth Biennial SGA-SEG Meeting Kraków. Lisse: Swets & Zeitlinger Publishers*, pp. 461-464.
- & — (in press). Plagioclase-mantled K-feldspar in the Carboniferous porphyritic microgranite of Altenberg-Frauenstein, eastern Erzgebirge/Krusne Hory. *Bulletin of the Geological Society of Finland*, **73** (2).
- NAREBSKI, W. 1994. Lower to Upper Paleozoic tectonomagmatic evolution of NE part of the Bohemian Massif. *Zentralblatt für Geologie und Paläontologie*, **9/10**, 961-972.
- NEKVASIL, H. & BURNHAM, C. W. 1987. The calculated individual effects of pressure and water content on phase equilibria in the granite system. In: B. O. MYSEN (Ed.), *Magmatic Processes: Physicochemical Principles*. University Park, Pa.: Geochemical Society, p. 500.
- NEKVASIL, H. 1991. Ascent of felsic magmas and formation of rapakivi. *American Mineralogist*, **76**, 1279-1291.
- OBERC-DZIEDZIC, T. 1985. The influence of Karkonosze granite on Izera gneisses. *Kwartalnik Geologiczny*, **29**, 571-588. [*In Polish*]
- OLIVER, G.J.H., CORFU, F. & KROGH, T.E. 1993. U-Pb ages from SW Poland: evidence for a Caledonian suture zone between Baltica and Gondwana. *Journal of the Geological Society*, **150**, 355-69.
- PATOČKA, F., FAJST, M. & KACHLIK, V. 2000. Mafic-felsic to mafic-ultramafic Early Palaeozoic magmatism of the West Sudetes (NE Bohemian Massif): the South Krkonose complex. *Zeitschrift Geologischen Wissenschaften*, **28**, 177-210.
- RÄMÖ & HAAPALA, 1995. One hundred years of Rapakivi Granite. *Mineralogy and Petrology*, **52**, 129-185.
- RAMSEYER, K., ALDAHAN, A.A., COLLINI, B. & LANDSTRÖM, O. 1992. Petrological modifications in granitic rocks from Siljan impact structure: evidence from cathodoluminescence. *Tectonophysics*, **216**, 195-204.
- RAMSEYER, K. & MULLIS, J. 2000. Geologic application of cathodoluminescence of silicates. In: PAGEL & *al.* (Eds), *Cathodoluminescence in geosciences*, pp. 177-192, *Springer*; Berlin.
- RUMBLE, D. 1976. The adiabatic gradient and adiabatic compressibility. *Carnegie Institution of Washington Year Book*, **75**, 651-655. Washington.

